Activity-Based Probes Hot Paper

Deutsche Ausgabe: DOI: 10.1002/ange.201602666
Internationale Ausgabe: DOI: 10.1002/anie.201602666

Activity-Based Proteome Profiling Probes Based on Woodward's Reagent K with Distinct Target Selectivity

Yong Qian, Marc Schürmann, Petra Janning, Christian Hedberg, and Herbert Waldmann**

Abstract: *Woodward's reagent K (WRK) is a reactive heterocyclic compound that has been employed in protein chemistry to covalently and unspecifically label proteins at nucleophilic amino acids, notably at histidine and cysteine. We have developed a panel of WRK-derived activity-based probes and show that surprisingly and unexpectedly, these probes are fairly selective for a few proteins in the human proteome. The WRK-derived probes show unique reactivity towards the catalytic N-terminal proline in the macrophage migration inhibitory factor (MIF) and can be used to label and, if equipped with a fluorophore, to image MIF activities in living cells.*

In activity-based proteome profiling (ABPP), probes with balanced, and often attenuated, chemical reactivity are employed to covalently bind, isolate, and identify proteins with enzymatic activity based on their mechanisms of action. Typically, a nucleophile in the enzyme active site reacts with an electrophile embedded in a selective probe. The final selectivity profile of a probe is often a combination of the relative electrophilicity of the binding site and the identity of the scaffold. A variety of different electrophiles have successfully been employed in ABPP probes.[1]

Woodward's reagent K (WRK; Figure 1 A)[2a] is a classical electrophile employed in protein chemistry to covalently bind to nucleophilic amino acids, notably cysteine and histidine.[2b–d] Mechanistically, WRK has been suggested to undergo a base-induced ring-opening reaction, forming a ketenimine intermediate, which subsequently traps a nucleophile (Figure 1 B).[2a,b,e] WRK or analogues thereof have thus far not been explored as ABPP probes of the human proteome, although WRK has been reported to irreversibly inactivate a number of enzymes in vitro.[2e] Herein, we describe that ABPP probes based on WRK are surprisingly selective reagents that target the macrophage migration inhibitory factor (MIF) by covalently modifying its catalytic N-terminal proline and can be employed to label and, if equipped with a fluorophore, to image MIF activities in living cells.

The probes that were synthesized for the affinity enrichment of proteins contained the reactive isoxazolium warhead of WRK and a terminal alkyne handle interconnected via an aromatic moiety and a spacer (Figure 1 A). The analytical workflow consists of the following steps (Figure 1 C): 1) Proteins are labeled with the ABPP probe, 2) an azide–biotin reporter tag (e.g., TAMRA–Biotin–N_3)[3] is added in a [3+2] cycloaddition, 3) affinity enrichment using a streptavidin solid support is performed, and 4) detection is done by 4a) SDS-PAGE/in-gel fluorescence scanning and/or 4b) tryptic digest and nano-HPLC MS/MS analysis. The probes **P1**–**P10** (Figure 1 D; for their complete structures, see the Supporting Information, Figure S1) and a negative control probe (NP) were synthesized by analogy according to established methods (see the Supporting Information).

The WRK probes **P1**–**P3**, with terminal alkyne linkers attached to different positions of the aromatic moiety (*ortho*, *meta*, or *para*), were incubated at different concentrations with HeLa cell lysate. Analysis of the resulting labeled proteome using in-gel fluorescence detection (see the Supporting Information for experimental details) revealed a major fluorescent band at 15 kDa (Figure 2 A, left panel), with an intensity that depended on the concentration of the probe and the substitution pattern of the aromatic ring in **P1**–**P3**. The influence of the probe substitution pattern was further ascertained with the isoxazolium salts **P4**–**P6** (Figure 2 A; for the structures, see Figures 1 D and S1), and the impact of the N substituent was determined by employing the probes **P7**–**P10** (Figure 2 A; for the structures, see Figures 1 D and S1) with an alkyne PEG handle. The *ortho*-substituted probes **P5** and **P6** showed a lower labeling efficiency than **P4**, suggesting that *ortho* modification decreased the interaction between probe and protein. **P8**, which contains a *meta*-substituted alkyne PEG handle and an *N*-ethyl isoxazolium core, showed the highest reactivity. Whereas in the presence of an *N*-butyl group (**P9**), the reactivity was comparable, the introduction of a methyl group (**P7**) or a cyclohexanemethyl group (**P10**) attenuated the reactivity (Figure S2 A). The labeling reaction was very fast, and a cell lysate could be efficiently labeled with **P8** even within 1 min incubation (Figure S2 B). Labeling was strongly diminished after heat denaturation, suggesting that the labeling reaction needs the intact proteome (Figure S2 C). Interestingly, the probes could be used over a wide pH range (pH 4.0–9.0; Figure S3).

P2- and **P8**-bound proteins were identified by proteomic analysis after probe ligation, pull down, and in-gel as well as on-bead[4] tryptic digestion. Table 1 shows the hit frequencies of proteins after in-gel digestion of the 15 kDa band for

[*] Dr. Y. Qian, Dr. M. Schürmann, Dr. P. Janning, Prof. Dr. H. Waldmann
Max Planck Institute of Molecular Physiology
Otto-Hahn-Strasse 11, Dortmund (Germany)
E-mail: herbert.waldmann@mpi-dortmund.mpg.de
Prof. Dr. C. Hedberg
Department of Chemistry, Chemical Biology Centre (KBC)
Umeå University, 90187 Umeå (Sweden)
E-mail: christian.hedberg@umu.se
Prof. Dr. H. Waldmann
Technical University Dortmund
Department of Chemistry and Chemical Biology
Otto-Hahn-Strasse 6, Dortmund (Germany)

Supporting information for this article can be found under: http://dx.doi.org/10.1002/anie.201602666.

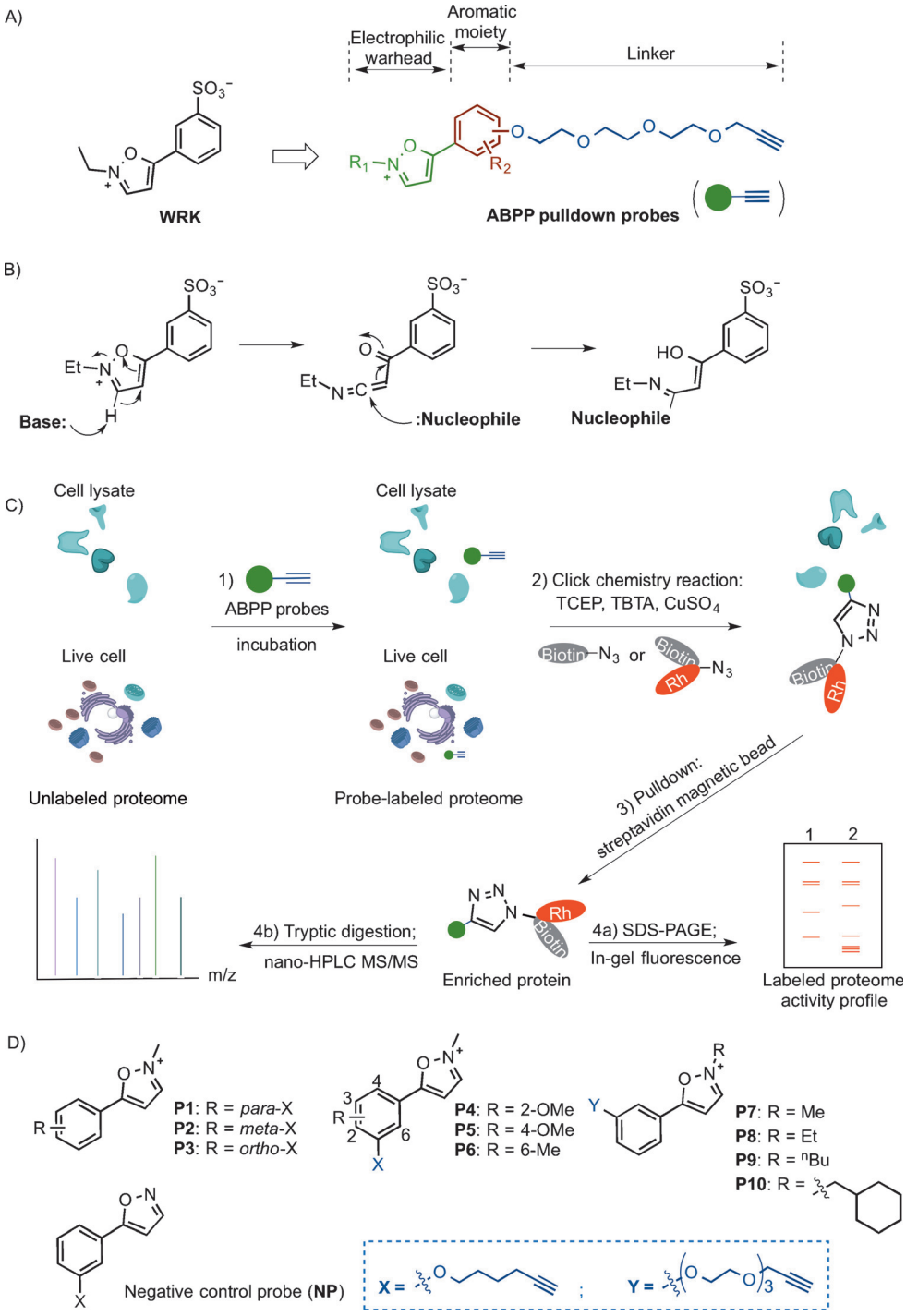

Figure 1. Design of WRK probes. A) General structure of the WRK probes. B) Base-induced reaction between WRK and nucleophiles as suggested by Woodward. C) Detection and identification of probe-labeled proteome by the ABPP strategy. D) Chemical structures of probes **P1**–**P10** (see the Supporting Information for the syntheses and the complete structures). TBTA = tris[(1-benzyl-1*H*-1,2,3-triazol-4-yl)methyl]amine, TCEP = tris(2-carboxyethyl)phosphine.

compound **P2**. MIF was the only protein identified as a hit in four independent replicates, which was further validated by Western blot analysis after pull down (Figure 2B). Affinity enrichment experiments using **P2** or **P8** as baits and on-bead digestion showed that the probes bind several other proteins as well, but most of them to a lower extent (Tables S1 and S2). MIF was also enriched in control experiments with cell lysates from HeLa, HEK293, and MCF-7 cell lysates when **P8** was used, whereas it was not detected when DMSO or the negative probe NP served as the control (Figure S4).

Pre-incubation of HeLa cell lysate with WRK (5/25 equiv, 100 μM/500 μM, 15 min) prior to the addition of 20 μM **P8** efficiently inhibited the labeling of MIF after pull down (Figure 2B), thus suggesting that WRK competes with **P8** for the same binding site in the same target. **P8** labeling of MIF can also be prevented with the WRK derivatives **PA** and **PBr** (Figure 2C; for the structures, see Figures 1D and S1), and pretreatment with the covalent MIF inhibitor **4-IPP**[5] (Figure 2C) fully blocked the labeling of MIF with **P8**. In contrast, **P8**-labeled proteins remained unchanged after treatment with the non-covalent MIF inhibitor **ISO-1** (Figure 2C).

MIF is a widely expressed cytokine that plays crucial physiological roles in immune and inflammatory responses.[6] Upon stimulation, MIF is released and further promotes the production of inflammatory mediators, such as TNF and IL-1.[7] An elevated level of MIF is associated with inflammatory and autoimmune disease and tumor growth.[6,8] Thus MIF has the potential to serve as a biomarker and therapeutic target.[9] MIF is a keto–enol tautomerase,[5,10] and can be inhibited with either the competitive inhibitor ISO-1[11] or with the covalent inhibitor **4-IPP**, which directly targets the catalytically active N-terminal proline residue.[5] Furthermore, isothiocyanates, as well as aminophen metabolites, have also been reported to inhibit MIF.[12]

Analysis of the WRK derivatives in a WST-1 proliferation assay indicates that the WRK probe is only weakly cytotoxic even at 100 μM (Figure S5). Cell permeability was confirmed

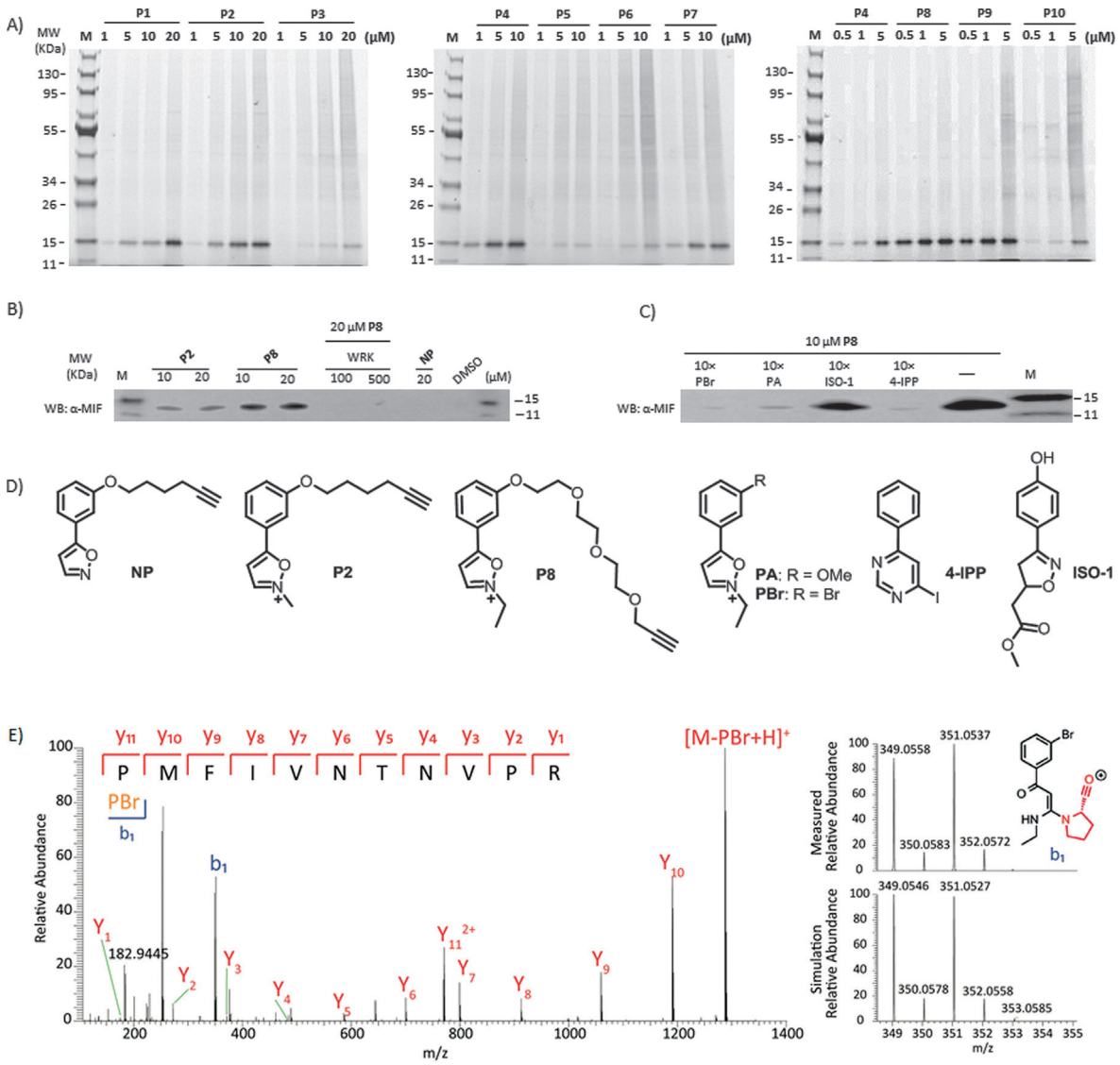

Figure 2. In vitro reactivity of WRK probes. A) Concentration-dependent in vitro labeling with representative WRK probes in HeLa cell lysates (10 min, 25 °C, pH 7.4), tagged with the TAMRA azide using click chemistry, and separated by SDS-PAGE. In-gel fluorescence scanning experiments were performed with the ChemDoc ™MP system (Bio-Rad). Fluorescent gel images shown in gray. MW = molecular weight. B) Confirmation of the major fluorescent band as MIF by Western blot analysis against a specific anti-MIF antibody, analysis after pull down on streptavidin beads and after competition with WRK. C) In vitro competitive labeling of MIF with **P8**; HeLa cell lysates were pre-incubated with different inhibitors (100 μM of the MIF inhibitors **4-IPP** and **ISO-1** or the WRK derivatives **PA** and **PBr**; 10 min) and then incubated with 10 μM **P8** for another 10 min; analysis by Western blot after pull down. D) Structures of the probes **NP**, **P2**, and **P8**, the WRK derivatives **PA** and **PBr**, and the MIF inhibitors **4-IPP** and **ISO-1**. E) Binding site of **PBr**. MIF (5 μL, 0.7 μg μL^{-1}) was incubated with 100 μM **PBr** in PBS buffer (pH 7.4) for 10 min at 25 °C. After acetone precipitation, MIF was digested with GluC and Trypsin. The resulting peptides were detected by nanoHPLC-MS/MS and analyzed with MaxQuant to identify the modification sites. Left: MS/MS spectrum of $m/z = 770.85$. Most peaks could be assigned to the full y ion series of the N-terminal peptide of MIF (Pro1 to Arg11) carrying the probe **PBr** bound to proline 1 (Pro1). Right: Enlarged region of the MS/MS spectrum for the fragment of proline 1 bound to the probe **PBr** (b_1 ion). The simulated isotope pattern of this fragment is shown below.

by the incubation of HeLa cells with Rhodamine-tagged **P8** (Figure 3 A) and co-localization of **P8** with MIF by two-color immunofluorescence analysis of these cells with a fluorescently labeled anti-MIF antibody (Figures 3 A and S6). The labeling efficacy in intact cells depends on the probe structure in the same manner as shown for the lysate experiments (Figures S7–S9), and the immunofluorescence staining intensity for probes **P8** and **P2** behaves accordingly (Figure S6). Labeling was abolished upon treatment of cells with MIF inhibitors prior to **P8** incubation (**4-IPP**, **PBr**; Figure S9). These observations suggest that the observed TAMRA fluorescence signal reflects the selective targeting of MIF by **P8** even in intact cells.

Based on these findings, we synthesized a probe suitable for the direct imaging of MIF in cells. The fluorescent probe **TP** (Figure 3 E) consists of a WRK reactive group bound to a naphthalene ring[13] (see the Supporting Information for its synthesis). Consequently, it could be reactive towards nucle-

Table 1: Hit frequency of proteins after four independent affinity enrichments and in-gel tryptic digestion of the 15 kDa band using compound **P2** as the bait.[a]

Protein	Gene	M_w [kDa]	Frequency
Macrophage migration inhibitory factor	MIF	12.476	4
Thioredoxin	TXN	11.737	3
Galectin-1	LGALS1	14.716	3
Protein S100-A16	S100A16	11.801	3
Protein S100-A4	S100A4	11.728	3

[a] Proteins identified as hits in at least three out of four experiments are listed. Hit definition: The protein is identified with at least two unique peptides in the compound sample after affinity enrichment, the overall intensity of the peak areas of the peptides belonging to the protein is greater than 1×10^8, and the intensity of the protein after affinity enrichment using the compound bait is at least ten times higher than the intensity of the same protein in the corresponding negative control (or the protein is not identified in the control).

ophilic residues in the active site of MIF. **TP** shows bright fluorescence and low cytotoxicity (Figures S10 and S11). After treatment of HeLa cells with 100 μM **TP** for two hours, confocal fluorescence microscopy imaging in the probe channel ($\lambda_{ex}=405$ nm) showed a strong fluorescence signal for **TP** treated cells, but not for cells treated with the corresponding negative control probe (**NTP**; Figure 3B). To investigate whether **TP** can detect the known upregulation of MIF by lipopolysaccharides (LPS),[14] we pretreated HeLa cells with 1 μg mL^{-1} LPS for 24 hours. After **TP** addition, LPS-treated cells showed a much stronger fluorescence signal than the control (Figure 3C). We transfected HeLa cells with MIF siRNA to silence the MIF gene. Here, a significant decrease in the blue fluorescence signals compared with the siRNA control group was observed (Figure 3C), thus indicating that **TP** may serve as an imaging probe to detect the up/downregulation of endogenous MIF in living cells.

To enable the live-cell imaging and subsequent in situ profiling of endogenous MIF by gel-based ABPP, a dual-purpose activity-based probe (**TPP**; for its structure, see Figure 3E) was developed. This probe is based on the same structure as **TP** and contains the same alkyne handle as structures **P7** to **P10**. All control experiments yielded similar

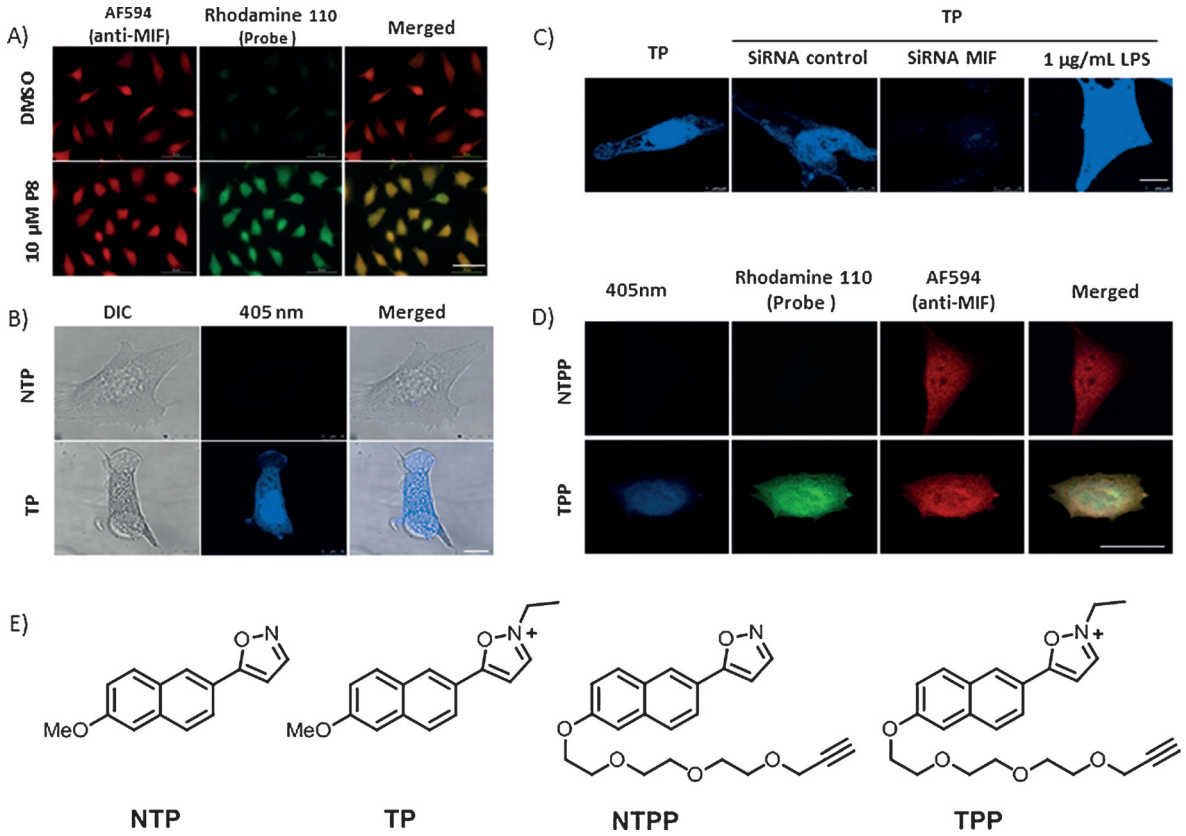

Figure 3. A) Immunofluorescence staining of HeLa cells with **P8**. HeLa cells were treated with **P8** (10 μM) or DMSO for 2 h at 37 °C. Then, the cells were fixed, permeabilized, and tagged with the Rhodamine110 azide using click chemistry; MIF was stained with a specific anti-MIF antibody. Two-color immunofluorescence analysis showing the significant colocalization of **P8**-tagged Rhodamine110 with MIF. Scale bar: 50 μm. B) Confocal fluorescence microscopy imaging of living HeLa cells with **TP** and the negative-control probe **NTP** (100 μM, 2 h). C) Images of HeLa cells with **TP** (100 μM, 2 h) with or without LPS (1 μg mL^{-1}, 24 h pretreatment), or the universal scrambled negative controls SiRNA or SiRNA MIF (100 nM, 48 h pretreatment). One-photon image ($\lambda_{ex}=405$ nm) for the **TP** probe. Scale bar: 10 μm. D) Images of HeLa cells with **TPP** or **NTPP** (100 μM, 2 h, 37 °C). One-photon images ($\lambda_{ex}=405$ nm) for the various probes; **TPP** was tagged with the Rhodamine110 azide using click chemistry; MIF immunofluorescence staining with a specific anti-MIF primary antibody and an Alexa Fluor 594 conjugated secondary antibody. Merged image of the three channel images. Scale bar: 25 μm. E) Chemical structures of the probes **NTP**, **TP**, **NTPP**, and **TPP**.

results as described for the structures mentioned above: 1) Concentration-dependent labeling showed that 500 nM **TPP** was sufficient for acquiring a significant fluorescence signal (Figure S12), 2) the enrichment of MIF was confirmed by immunoblot analysis after labeling of cell lysate and intact cells with **TPP** after pull down (Figures S13 and S14), 3) pretreatment of cell lysate with 100 μM **TP**, **PA**, **PBr**, **4-IPP**, or WRK completely abolished the labeling by **TPP** (Figure S15), and 4) pretreatment of the HeLa cells with inhibitors (100 μM **4-IPP** or **TP** for 2 h) significantly decreased the labeling of MIF by **TPP** (Figure S14).

To confirm the suitability of **TPP** for live-cell imaging, HeLa cells were incubated with **TPP** and imaged in the probe channel ($\lambda_{ex} = 405$ nm) by confocal fluorescence microscopy, accompanied by three-color immunofluorescence with Rhodamine110 tagged to the alkyne and immunoblotting with anti-MIF antibodies. **TPP**-treated cells showed a strong fluorescence signal (Figure 3D), clearly co-localized with the MIF signal. These findings suggest that **TPP** enables the visualization of MIF activity in live cells in combination with the affinity enrichment of labeled proteins.

Experiments using recombinant MIF enabled the identification of the reactive amino acid residue. Mass-spectrometric analysis of intact MIF before and after the reaction with **P8** and pre-incubation with the MIF inhibitors **4-IPP** or **ISO-1** prior to **P8** labeling or incubation with **PA** showed mass shifts that corresponded to the desired products, indicating the expected covalent modifications of the protein (for the ESI-MS and MALDI/TOF-MS spectra, see Figures S16–S18). The labeling site was determined by LC-MS/MS analysis, after double digestion of recombinant MIF incubated with **4-IPP**, **PA**, **PBr**, and **P8** with GluC and trypsin. Proline 1 was identified as the primary site of modification (Figure 2E and Figure S19). Incubation of **TP** with proline, proline methyl ester, and *N*-acetyl-L-proline followed by LC-MS analysis clearly revealed the reaction of the probe with the secondary amine of proline (Figure S20).

Based on the knowledge that the N-terminal proline is the binding site targeted by the WRK-like probes, we investigated whether other proteins with an N-terminal proline were also enriched. However, a search in the pull-down lists against a list of proteins carrying an N-terminal proline (Table S3) showed no other significant enrichment of proteins from this subset of the proteome.

In summary, we have demonstrated that WRK-derived reactive probes open up new opportunities for proteome labeling and imaging both in vitro and in living cells. Surprisingly, despite their relatively simple structures and without elaborated probe design, the WRK derivatives selectively labeled the macrophage migration inhibitory factor (MIF) at its N-terminal proline. Given that elevated MIF activities are particularly associated with inflammatory and proliferative diseases,[6] the WRK-derived reagents described here, in particular **TP** and **TPP**, may serve as valuable functional reagents to unravel the role of MIF in the corresponding biological processes.

Acknowledgements

We thank the Max-Planck Society for generous support. Y.Q. is grateful to the Alexander von Humboldt Foundation for a postdoctoral fellowship. C.H. is grateful for generous support from the Knut and Alice Wallenberg Foundation (Sweden).

Keywords: activity-based probes · fluorescent imaging · protein labeling · proteomics

How to cite: *Angew. Chem. Int. Ed.* **2016**, *55*, 7766–7771
Angew. Chem. **2016**, *128*, 7897–7902

[1] a) M. Gersch, J. Kreuzer, S. A. Sieber, *Nat. Prod. Rep.* **2012**, *29*, 659–682; b) D. A. Shannon, E. Weerapana, *Curr. Opin. Chem. Biol.* **2015**, *24*, 18–26; c) M. J. Niphakis, B. F. Cravatt, *Annu. Rev. Biochem.* **2014**, *83*, 341–377.

[2] a) For the initial reports of WRK, see: R. B. Woodward, R. A. Olofson, H. Mayer, *J. Am. Chem. Soc.* **1961**, *83*, 1010–1012 and R. B. Woodward, R. A. Olofson, *J. Am. Chem. Soc.* **1961**, *83*, 1007–1009; b) P. Bustos, M. I. Gajardo, C. Gomez, H. Goldie, E. Cardemil, A. M. Jabalquinto, *J. Protein Chem.* **1996**, *15*, 467–472; c) A. R. Johnson, E. E. Dekker, *Protein Sci.* **1996**, *5*, 382–390; d) N. Carvajal, E. Uribe, V. Lopez, M. Salas, *Protein J.* **2004**, *23*, 179–183; e) K. Llamas, M. Owens, R. L. Blakeley, B. Zerner, *J. Am. Chem. Soc.* **1986**, *108*, 5543–5548.

[3] a) A. E. Speers, B. F. Cravatt, *Chem. Biol.* **2004**, *11*, 535–546; b) M. Rusch, T. J. Zimmermann, M. Burger, F. J. Dekker, K. Gormer, G. Triola, A. Brockmeyer, P. Janning, T. Böttcher, S. A. Sieber, I. R. Vetter, C. Hedberg, H. Waldmann, *Angew. Chem. Int. Ed.* **2011**, *50*, 9838–9842; *Angew. Chem.* **2011**, *123*, 10012–10016.

[4] M. Gersch, F. Gut, V. S. Korotkov, J. Lehmann, T. Böttcher, M. Rusch, C. Hedberg, H. Waldmann, G. Klebe, S. A. Sieber, *Angew. Chem. Int. Ed.* **2013**, *52*, 3009–3014; *Angew. Chem.* **2013**, *125*, 3083–3088.

[5] M. Winner, J. Meier, S. Zierow, B. E. Rendon, G. V. Crichlow, R. Riggs, R. Bucala, L. Leng, N. Smith, E. Lolis, J. O. Trent, R. A. Mitchell, *Cancer Res.* **2008**, *68*, 7253–7257.

[6] T. Calandra, T. Roger, *Nat. Rev. Immunol.* **2003**, *3*, 791–800.

[7] F. Bai, O. A. Asojo, P. Cirillo, M. Ciustea, M. Ledizet, P. A. Aristoff, L. Leng, R. A. Koski, T. J. Powell, R. Bucala, K. G. Anthony, *J. Biol. Chem.* **2012**, *287*, 30653–30663.

[8] a) E. F. Morand, M. Leech, J. Bernhagen, *Nat. Rev. Drug Discovery* **2006**, *5*, 399–410; b) E. J. Miller, J. Li, L. Leng, C. McDonald, T. Atsumi, R. Bucala, L. H. Young, *Nature* **2008**, *451*, 578–582; c) H. Conroy, L. Mawhinney, S. C. Donnelly, *QJM* **2010**, *103*, 831–836; d) L. Xu, Y. Li, H. Sun, X. Zhen, C. Qiao, S. Tian, T. Hou, *Drug Discovery Today* **2013**, *18*, 592–600.

[9] a) H. Ouertatani-Sakouhi, F. El-Turk, B. Fauvet, M. K. Cho, D. P. Karpinar, D. Le Roy, M. Dewor, T. Roger, J. Bernhagen, T. Calandra, M. Zweckstetter, H. A. Lashuel, *J. Biol. Chem.* **2010**, *285*, 26581–26598; b) L. Xu, Y. Zhang, L. Zheng, C. Qiao, Y. Li, D. Li, X. Zhen, T. Hou, *J. Med. Chem.* **2014**, *57*, 3737–3745; c) P. Dziedzic, J. A. Cisneros, M. J. Robertson, A. A. Hare, N. E. Danford, R. H. Baxter, W. L. Jorgensen, *J. Am. Chem. Soc.* **2015**, *137*, 2996–3003.

[10] S. L. Stamps, M. C. Fitzgerald, C. P. Whitman, *Biochemistry* **1998**, *37*, 10195–10202.

[11] J. B. Lubetsky, A. Dios, J. Han, B. Aljabari, B. Ruzsicska, R. Mitchell, E. Lolis, Y. Al-Abed, *J. Biol. Chem.* **2002**, *277*, 24976–24982.

[12] a) For the use of isothiocyanates as MIF inhibitors, see: J. V. Cross, J. M. Rady, F. W. Foss, C. E. Lyons, T. L. Macdonald, D. J.

Templeton, *Biochem. J.* **2009**, *423*, 315 – 321 and J. D. Tyndall, H. Lue, M. T. Rutledge, J. Bernhagen, M. B. Hampton, S. M. Wilbanks, *Acta Crystallogr. Sect. F* **2012**, *68*, 999 – 1002; b) for the use of aminophen derivatives as MIF inhibitors, see: P. D. Senter, Y. Al-Abed, C. N. Metz, F. Benigni, R. A. Mitchell, J. Chesney, J. Han, C. G. Gartner, S. D. Nelson, G. J. Todaro, R. Bucala, *Proc. Natl. Acad. Sci. USA* **2002**, *99*, 144 – 149.

[13] Y. Liu, X. Zhang, Y. L. Tan, G. Bhabha, D. C. Ekiert, Y. Kipnis, S. Bjelic, D. Baker, J. W. Kelly, *J. Am. Chem. Soc.* **2014**, *136*, 13102 – 13105.

[14] a) R. L. Damico, A. Chesley, L. Johnston, E. P. Bind, E. Amaro, J. Nijmeh, B. Karakas, L. Welsh, D. B. Pearse, J. G. Garcia, M. T. Crow, *Am. J. Respir. Cell Mol. Biol.* **2008**, *39*, 77 – 85; b) O. Flieger, A. Engling, R. Bucala, H. Lue, W. Nickel, J. Bernhagen, *FEBS Lett.* **2003**, *551*, 78 – 86.

Received: March 16, 2016
Published online: May 9, 2016

